Characterization of Power Optimizer Potential to Increase Energy Capture in Photovoltaic Systems Operating Under Non-Uniform Conditions

Sara MacAlpine
University of Colorado
1111 Engineering Drive, Boulder, CO 80309
sara.macalpine@colorado.edu

Robert W. Erickson, Fellow, IEEE
University of Colorado and Phobos Energy, Inc.

Michael J. Brandemuehl
University of Colorado

Special Issue on Power Electronics in Photovoltaic Applications, 2013

Abstract: Power optimizers, which perform power conversion and distributed maximum power point tracking (DMPPT) at the sub-array level, are available to mitigate losses associated with non-uniform operating conditions in grid-tied photovoltaic (PV) arrays, yet there is not good understanding of their potential to increase energy capture. This work develops and demonstrates a methodology for the use of a detailed software tool that can accurately model both partial shading and electrical mismatch at the sub-panel level in a PV array. Annual simulations are run to examine the device-independent opportunity for power recovery in arrays with light, moderate, and heavy shading, and sub-panel electrical mismatch variations based on measurements from a monocrystalline silicon array. It is found that in unshaded arrays, the potential energy gain is <1% using power optimizers, but in shaded arrays it increases to 3-16% for panel-level DMPPT and 7-30% for cell-level DMPPT. In the set of simulated cases, panel-level power optimization recovers 34-42% of the energy that is lost to partial shading.

I. INTRODUCTION

Small scale residential or commercial sized grid-tied photovoltaic (PV) systems have gained greater popularity in recent years, fueled by new, more flexible module designs and government and utility sponsored incentives favoring solar technologies. However, the complex designs and landscapes of PV systems in urban and suburban environments frequently bring about non-uniform operating conditions within the array, because of factors such as varied panel orientation, soiling, shading, or mismatched electrical characteristics between PV cells. When operating conditions are not uniform for a conventional, grid-tied array, constraints induced by the series/parallel connections cause portions to sacrifice their individual power production potential, and the system does not operate at its maximum possible efficiency. Nonuniformity-related power losses generally consist of a fixed and a recoverable component as depicted in Figure 1. The latter of these creates opportunities for sub-array power optimizers and distributed maximum power point tracking (DMPPT), shown in Figure 2, to increase energy capture throughout the year. Numerous authors [1-8] have studied the performance and optimization of different power optimizer designs, and there are many commercial products, both microinverters and DC-DC converters, [9] which allow for DMPPT in PV systems.
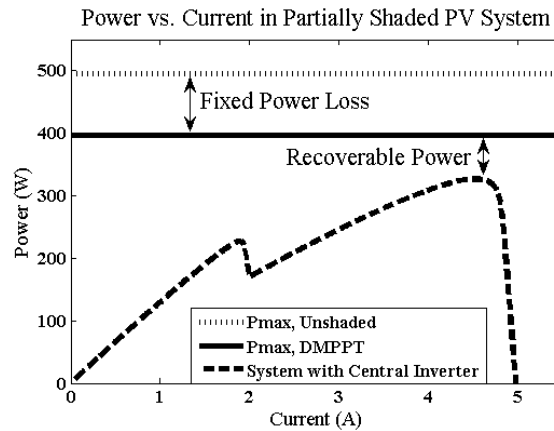
Figure 1 - Fixed and recoverable power losses in a partially shaded PV system

Despite the increased availability of power optimizers, little independent research is available quantifying the benefits that they can provide in realistic installation situations. Existing research mostly focuses on short term performance under specific conditions [10-13], which is a much less significant metric than annual energy impact. Though the author of [14] does include annual simulations of partial shading with and without power optimizers, they are performed using a simplified empirically-based method rather than modeling detailed array electrical

interactions, so the methodology is likely not directly applicable to other installations. In contrast [15] contains a very detailed mismatch modeling tool with annual energy simulation capability; however, the study's nonstandard assumptions about panel topology and array operating conditions lead to unrealistic predictions. Additionally, all of the works mentioned above assume a certain power optimizer architecture and design, which makes each set of results potentially device-specific.
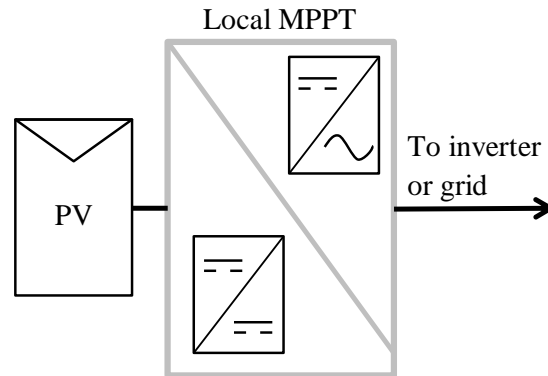
Figure 2 - Photovoltaics with distributed maximum power point tracking

Commercially available power optimizers have a wide range of design strategies and circuit topologies, and thus also have a wide range of operating regimes, efficiencies, and insertion losses. Furthermore, the designs are always evolving and improving, so study of a particular device may quickly become irrelevant as it is replaced by a new product. It therefore makes sense when studying the potential benefit of power optimizers to model them in a device-independent manner, as though they are capable of performing ideal DMPPT at different levels in the array. Results of simulations with this metric may be used by consumers and installers to understand when power optimizers should be considered, and based on this result they can then determine which device is best suited to their specific installations.

The purpose of this work is to describe an improved methodology for accurate prediction of partial shading and electrical mismatch related losses in PV arrays, and to use this methodology to demonstrate the potential for increased annual energy capture in a set of realistic PV systems employing DMPPT at various sub-array levels. This extends previous investigations on the subject [16] by adding electrical mismatch to the model and simulating a more realistic and diverse set of shading scenarios. Organization of the paper is as follows.

Section II reviews PV array performance with non-uniform operating conditions and discusses the ways in which they are modeled by the existing set of commercial PV simulation software. It is shown that accurate prediction of mismatch-related losses in PV systems (and thus potential for recoverable power using DMPPT) requires a more detailed approach than is currently available, motivating the development of a new simulation tool described in Section III. This tool allows cell-level modeling of partial shading and electrical mismatch in PV systems, using an improved version of the standard single diode PV generator model. Power optimizers are modeled as ideal DMPPT in order to investigate the maximum potential for their use, independent of any particular technology or device.

The annual simulations and types of mismatch that they address are described in Section IV. Electrical characteristics of each panel in a typical, mononcrystalline silicon array are measured at the sub-module level, and these varied characteristics are used to model inherent performance differences between sub-modules in the simulated cases. Realistic variation between PV generators in an array allows examination of the potential for increased energy capture using DMPPT in unshaded arrays, which are fairly common. In addition, partial shading is simulated for light, moderate, and heavy shading cases, which are derived from a survey of data from real PV installations.

Simulation results are presented and analyzed in Section V. Shading losses in conventional grid-tied PV systems are shown to vary with array configuration, confirming the necessity of detailed mismatch and shade modeling. Power optimizers show a small potential (<1%) for increased annual energy capture in unshaded arrays in both cloudy and sunny climates. Partially shaded arrays exhibit more potential: 3-16% for panel-level DMPPT and 7-30% for cell-level DMPPT. In each of the simulated cases panel-level power optimization recovers 34-42% of the energy that is lost to partial shading. Finally, Section VI concludes and summarizes the paper.

II. MISMATCHED PV SYSTEM PERFORMANCE

A typical residential or small commercial BIPV system configuration, consisting of one or more parallel strings of photovoltaic modules connected to the electrical grid through an inverter, is shown in Figure 3. The array operating point (voltage and current) is controlled by maximum power point tracking (MPPT) at the central inverter, with each PV generator (panel, cell, etc.) in a series string conducting the same current. Parallel strings may have differing currents, but each must have the same voltage potential across it.
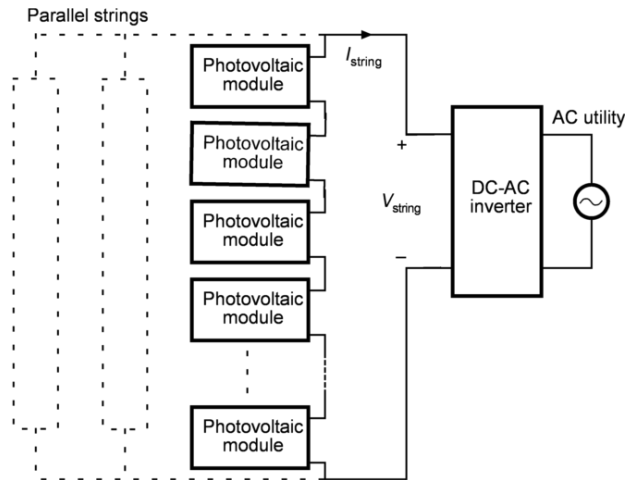
Figure 3 - Conventional grid-tied PV system

In an ideal system with no mismatch, PV generators exhibit the nonlinear performance characteristics found in Figure 4, but the system performance is nonetheless straightforward to model, as maximum power can be directly calculated from the single performance curve for any given incident irradiance and PV cell temperature.
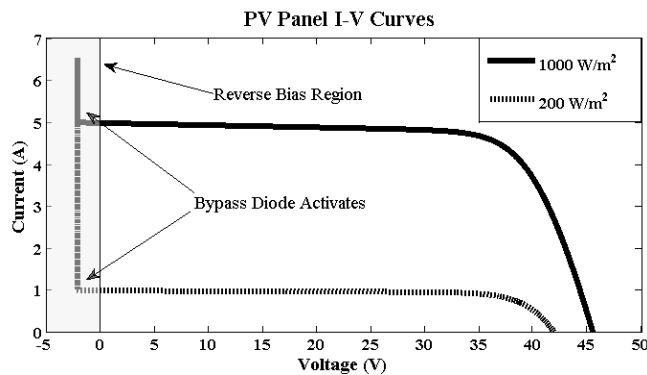

Figure 4 - Panel I-V curves at high and low irradiance

In a series string with mismatch, however, such as one including both unshaded and shaded PV panels, the unshaded panels will have a higher optimal power producing current. If the shaded panels in a string are forced to operate at the higher optimal current of the string's unshaded panels, which may exceed their short-circuit current (see Figure 4), it is likely that their cells will become reverse biased (negative voltage) and actually dissipate power rather than producing it. To limit power losses associated with this dissipation, and also to minimize heat damage, most PV panels have bypass diodes in their junction boxes, each serving a group of 12-24 cells, here referred to as a sub-module. These allow a string of modules to operate at the higher optimal (unshaded) current, bypassing the shaded

cells, but in this case any power that the bypassed cells could have produced at their lower optimal operating current is lost and string operating voltage decreases. In addition to series string effects, systems with parallel strings have added complexity which often leads to increased losses from shading: when shaded parts of the array are bypassed, the unshaded parts may be forced to either a) operate at a higher-than-optimal voltage to compensate for the bypassed areas or b) operate at a lower-than-optimal voltage to match strings with more extensive shading.

Accurate determination of potential for power optimizers' increased energy capture depends directly on correct modeling of PV systems with mismatch. The presence of bypass diodes in PV panels allows sub-module behavior variations which cannot be accounted for by merely averaging the incident irradiance over the panel. Figure 5 confirms that a module is often able to produce more power if the shading is isolated to just one sub-module. A survey of the most popular PV system simulation tools [17] shows that none model arrays with this level of detail, so they cannot accurately model the impact of shading/mismatch.

(a)

(b)
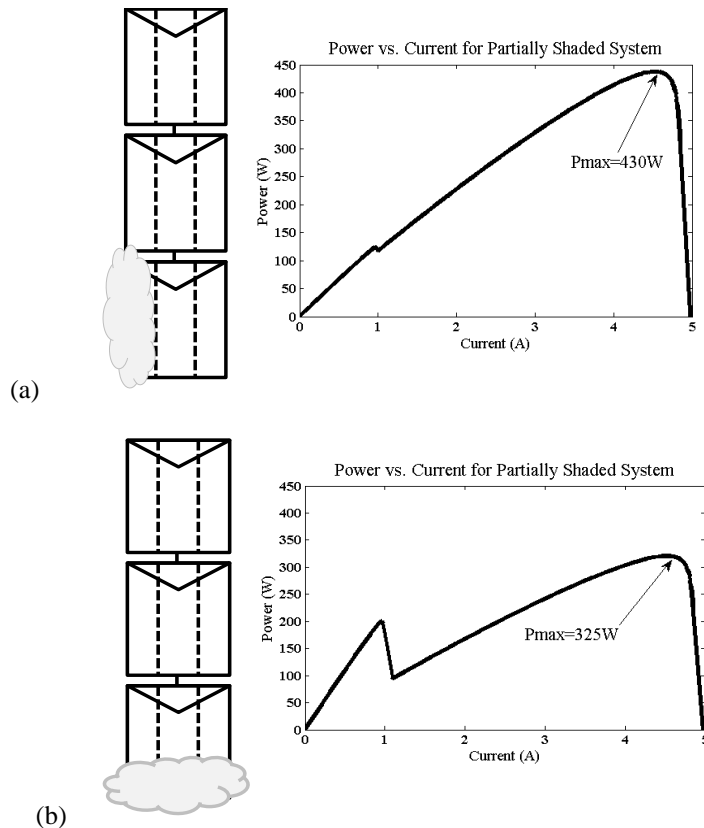
Figure 5 - Partial shading and system power for (a) shade isolated to one sub-module (sub-modules delimited by dashed lines) and (b) shading distributed across sub-modules

Instead, currently available PV modeling tools handle non-uniform conditions using simplified assumptions which are likely to sacrifice accuracy. In all of tools above, for instance, electrical mismatch between generators is modeled as constant, user-defined derate factor that often has no relation to the actual array performance. Partial array shading may be accounted for in different ways; some tools [18] do not include it at all, while others [19] require the user to independently generate and input hourly shade profiles. PVsyst [20], one of the most popular and detailed PV system modeling tools used in the U.S., bounds shading losses but does not accurately predict the impact of partial shading under most conditions as this would be too computationally intensive [21]. Even if these tools are able to model DMPPT well, they must model the initial mismatch-related losses correctly in order to achieve accurate comparison predictions with and without power optimizers. It is clear that to examine the potential for power optimizers' increased energy capture, a more detailed PV system model is needed.

III. DETAILED PV SYSTEM MODELING TOOL

Responding to the need described above, the authors have created a tool for the detailed annual simulation of PV system performance in the MATLAB environment. This tool allows modeling of partial shading and electrical mismatch at the PV cell level. Inputs include panel details (electrical parameters, dimensions, tilt and orientation, cell and bypass diode layout), array size (panels per row and number of rows) and configuration (single series string or division of parallel series strings). 3-D shading analysis requires inputs for the shading object's height, diameter, and position relative to the array, which are used to map shadows onto the array plane.

A. Hourly Operating Conditions

Hourly weather data (irradiance, ambient temperature, and wind speed) are taken from TMY3 data [22] for locations throughout the U.S. The incident irradiance on the array's tilted plane is made up of three components: beam, diffuse, and reflected, and the total is calculated using the HDKR anisotropic sky model, which accounts for circumsolar diffuse irradiance and horizon brightening. [23] Elements of the array shaded by opaque objects receive the reflected and non-circumsolar diffuse portions of the total available irradiance, as recommended in [24]. Those that are shaded by semi-transparent objects receive in addition a corresponding fraction of the beam and circumsolar diffuse portions. Each PV cell is divided into subcells, with the total available irradiance averaged over the cell to simulate instances with partial cell shading. The radiation absorbed by each PV cell is then calculated

from its incident irradiance and solar angles using Snell's, Fresnel's and Bougher's laws as well as air mass modifiers described in [23].

Hourly cell temperature is calculated using Sandia temperature model [25], which depends empirically on ambient temperature, wind speed, absorbed irradiance, and array mounting. A recent study [26] shows that this model is more accurate than others when modeling building mounted or building integrated PV arrays.

B. PV Generator Model

At the cell level, PV generators are modeled using the Wisconsin SEL 7 parameter single diode model, which is similar to the commonly-used 5 parameter diode model [23] but includes parameters that reflect module behavior under low irradiance conditions. [27] Equation 1 gives the main equation for this model, which is presented in Figure 6. In this equation, I_L is the light current, I_o is the diode reverse saturation current, R_s is the series resistance, R_{sh} is the shunt resistance, and a is the modified ideality factor. I and V are the generator's current and voltage, respectively.
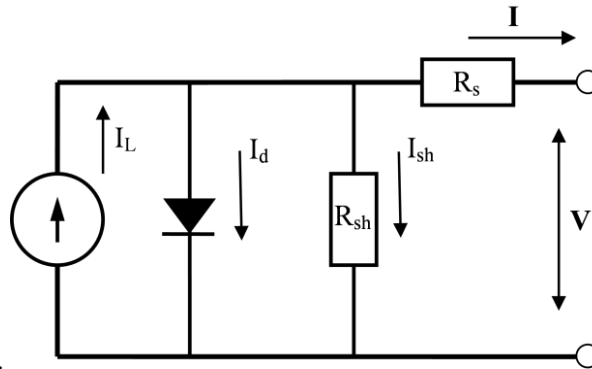

Figure 6 - Single diode model of PV generator

$$I = I_L - I_o \cdot \left[\exp\left(\frac{V + I \cdot R_s}{a}\right) - 1\right] - \frac{V + I \cdot R_s}{R_{sh}} \tag{1}$$

The five parameters, I_L, I_o, R_s, R_{sh}, and a are solved for at a reference point (often standard test conditions, STC = 1000 W/m^2 and 25°C) using information provided by the manufacturer's data sheet or measured data as detailed in [23]. With the five parameters solved for at reference conditions, they may then be converted to actual conditions

and used to find I-V curve characteristics. In the 7 parameter diode model, the parameter a varies only with temperature.

$$\frac{a}{a_{ref}} = \frac{T_{cell}}{T_{cell,ref}}$$

(2)

The light generated current I_L varies with absorbed irradiance, S, and also the short current temperature coefficient $\mu_{I,sc}$, which is given by the manufacturer

$$I_L = \frac{S}{S_{ref}} \cdot \left[I_{L,ref} + \mu_{I,sc} \cdot \left(T_{cell} - T_{cell,ref}\right)\right]$$

(3)

Shunt resistance R_{sh} varies with absorbed irradiance in the model.

$$\frac{R_{sh}}{R_{sh,ref}} = \frac{S_{ref}}{S}$$

(4)

In the 7 parameter model [27] R_s is allowed to vary with temperature relative to reference conditions. The associated δ parameter (6th parameter in the 7 parameter model) is found using the manufacturer-provided coefficient for temperature dependence of the maximum power point.

$$R_s|_T = R_{s,ref} \cdot \exp(\delta \cdot \Delta T)$$

(5)

Finally, I_0 is allowed to vary with both temperature and irradiance in the 7 parameter model. The m parameter (7th parameter in the 7 parameter model) is found using the module's maximum power current and voltage at low irradiance, which can be measured or manufacturers are required to provide according to CEC guidelines and the new IEC 61853 standard [28]. In the equation below, Eg is the material bandgap energy and k is Boltzmann's constant.

$$I_0 = I_{0,ref} \cdot \left(\frac{S_{ref}}{S}\right)^m \left(\frac{T}{T_{ref}}\right)^3 \exp\left(\frac{Eg_{ref}}{k \cdot T_{ref}} - \frac{Eg}{k \cdot T}\right)$$

(6)

Use of the 7-parameter model was found to dramatically increase model accuracy at low irradiance as compare to the 5 parameter model for a variety of PV module technologies [29]. Comparison of the model to measured I-V

curve data at low and high irradiance for a typical monocrystalline sub-module (see Figure 7) shows a good fit, especially around the maximum power point.

I-V Curve for Sub-Module 2 in Panel 21
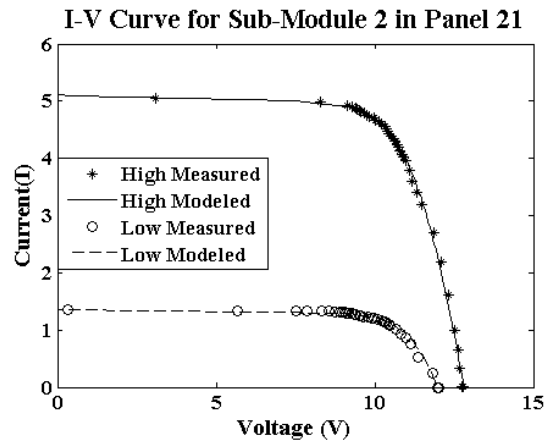
Figure 7 - Comparison between measured I-V curves and those fitted with the 7-parameter single diode model

C. Other System Component Models

All of the PV system's panels have a user-input number of bypass diodes, each with an assumed forward voltage drop of 0.7V. The simulations in this work focus on system DC (pre-inverter) power, with the string voltage constrained to a typical MPPT input voltage range for central inverters, 250-480V [30]. Simulations of arrays including power optimizers model them simply as ideal DMPPT, to better illustrate the maximum potential for increased energy capture.

IV. SIMULATED CASES

Annual simulations are run using TMY3 data for Boulder, Colorado (sunny climate), Orlando, Florida (cloudy climate). In all cases the modeled array is oriented due south, with a 22.6 degree (5:12 roof pitch) tilt, illustrated in Figure 8. The simulated arrays are made up of twenty-four 180W monocrystalline panels, each with three bypass diodes, arranged in two parallel strings of twelve panels. This array configuration was chosen for simulation as it was found to be one of the most common configurations in a survey of California PV systems. [31]
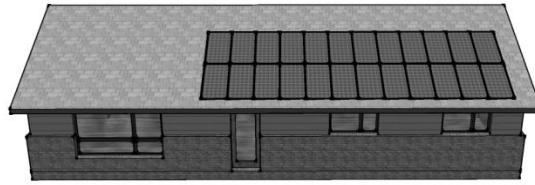
Figure 8 - Simulated array

A. Electrical Mismatch

All PV systems experience some degree of mismatched electrical characteristics between their panels/cells, which arise from manufacturing tolerances, defects, or degradation. In spite of the increased availability of power optimizers and sub-array DMPPT, little work has been done to quantify the potential that electrical mismatch creates for increased energy capture. One investigation of electrical mismatch using an indoor simulator [32] showed system gains of up to 5% under certain conditions, but the authors acknowledge that the variability of their lamps may have contributed to the results. There are few recent studies of electrical mismatch in field-deployed PV systems, and none which model mismatch at the sub-module level.

This work's simulations include modeling of electrical mismatch at the sub-module level, using data collected from a 4kW array of 24 monocrystalline modules mounted on a roof at the University of Colorado Boulder. The tested array is shown in Figure 9a. In order to record sub-module data, a custom printed circuit board (PCB) with a microcontroller and bypass diode level voltage sensors (Figure 9b) was designed and mounted in each panel's junction box. These PCBs allow collection of rapid, concurrent voltage measurements from each sub-module.

(a)

(b)
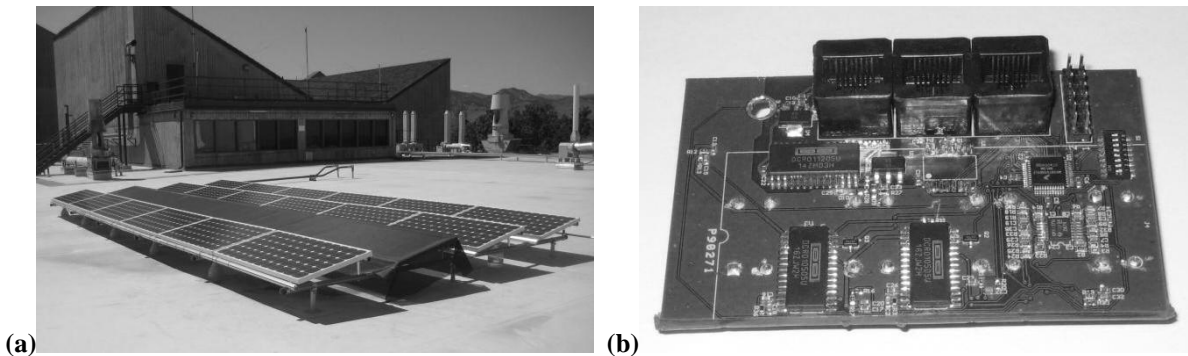
Figure 9 - (a) University of Colorado PV array and (b) PCB for sub-module data collection

Panels were connected in series with a programmable DC load in order to sweep I-V curves of multiple array elements simultaneously. I-V curves were taken under high (~1000 W/m^2) and low (~250 W/m^2) irradiance conditions, with in-plane irradiance measured by pyranometers calibrated at the National Renewable Energy Laboratory, and cell temperature measured using several type-T thermocouples mounted on the panels' back sides. The high and low irradiance I-V curves were recorded around solar noon on sunny days to decrease temporal irradiance variability; low irradiance conditions were achieved using a 75% opaque black mesh [33] shown in Figure 9a.

The measured I-V curves for each sub-module were fitted to the 7-parameter diode model using methods described in [34] with high and low light fit shown previously in Figure 7. A separate diode model for each sub-module is included in the simulations. It should be noted that while the fit was generally good for most sub-modules, there is some room for improvement particularly for PV generators which exhibit slightly "nonstandard" I-V curves. Figure 10 illustrates the modeled power vs. current curves under standard test conditions (1000 W/m^2, 25°C) and standard low irradiance conditions (200 W/m^2, 25°C). While most of the sub-modules have similar maximum power point currents, there are a few that are lower than the rest at both high and low irradiance; these outliers create more opportunity for power optimizers in series strings.
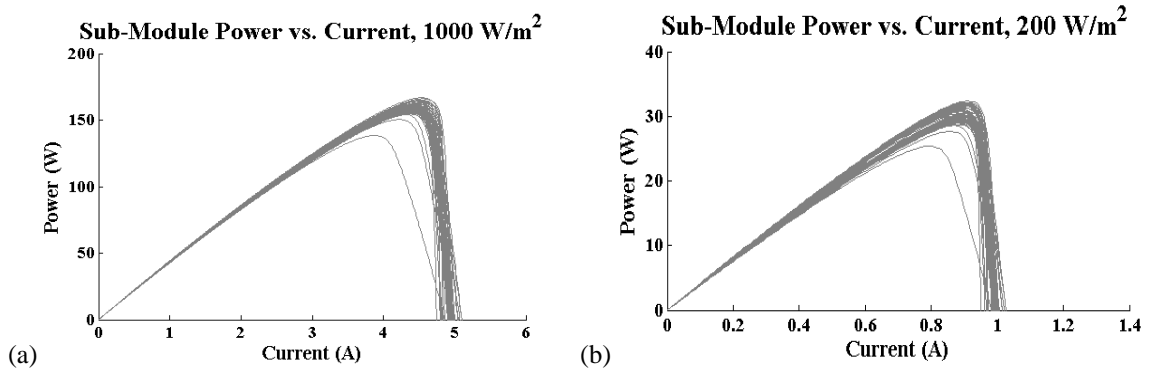
Figure 10 - Sub-module power curves at (a) high irradiance and b) low irradiance

The variations observed between sub-modules on the University of Colorado array and included in this work's simulations are assumed to be typical for newer, less expensive monocrystalline modules, which are very commonly used in PV installations in the U.S. Electrical mismatch may vary with degradation or panel type, which could create more or less opportunity for power optimizers and DMPPT.

B. Partial Shading

Shading cases for simulation were chosen based on a survey of Solmetric solar access data for installed PV sites described in [35]. Solmetric solar access (the percent of incident irradiance that is available to the array throughout the year) is calculated using sun paths and fish-eye images taken at key points in the array, with the assumption that any part of the array that is shaded at any time receives no radiation. According to the distribution of survey results, "light" shading corresponds to a 5-15% loss of solar access over the year, "moderate" is 15-20%, and "heavy" is any solar access loss greater than 20%.

The definition of solar access loss is slightly different for these simulations, because 1) the shadows are directly mapped onto the array for every hour during the year and 2) shaded portions of the array do receive the diffuse irradiance fraction. In this work the solar access loss is defined in Equation 7. The cases to be simulated were chosen such that if shade is modeled without receiving the diffuse light fraction, the percent solar access loss falls into the previously-defined (by Solmetric standards) light, moderate, or heavy shading categories indicated in the installer data.

$$\text{Solar Access Loss} = 1 - \frac{\text{Total Annual Insolation with Shading}}{\text{Total Annual Unshaded Insolation}} \qquad (7)$$

Each of the simulated shading scenarios, illustrated in Figure 11, is modeled after actual residential installations in the southwest United States. Shading obstacles include chimneys, pine trees, and deciduous trees. Chimneys and pines are modeled as fully opaque cylinders throughout the year. Deciduous trees are modeled as cylinders containing a number of fully opaque cylindrical "branches" surrounded by leaves. The "leaf" portions of the cylinder are assumed to have varying transparencies, following a normal distribution. During the warmer seasons, the leaf distribution is centered at 20% transparent, and during the winter it is centered at 75% transparent to account for leaf drop. Examples of the shadows mapped onto the array plane at the cell level are shown in Figure 12. An unshaded case is also simulated to investigate the potential for increased energy capture in arrays with no appreciable shading.
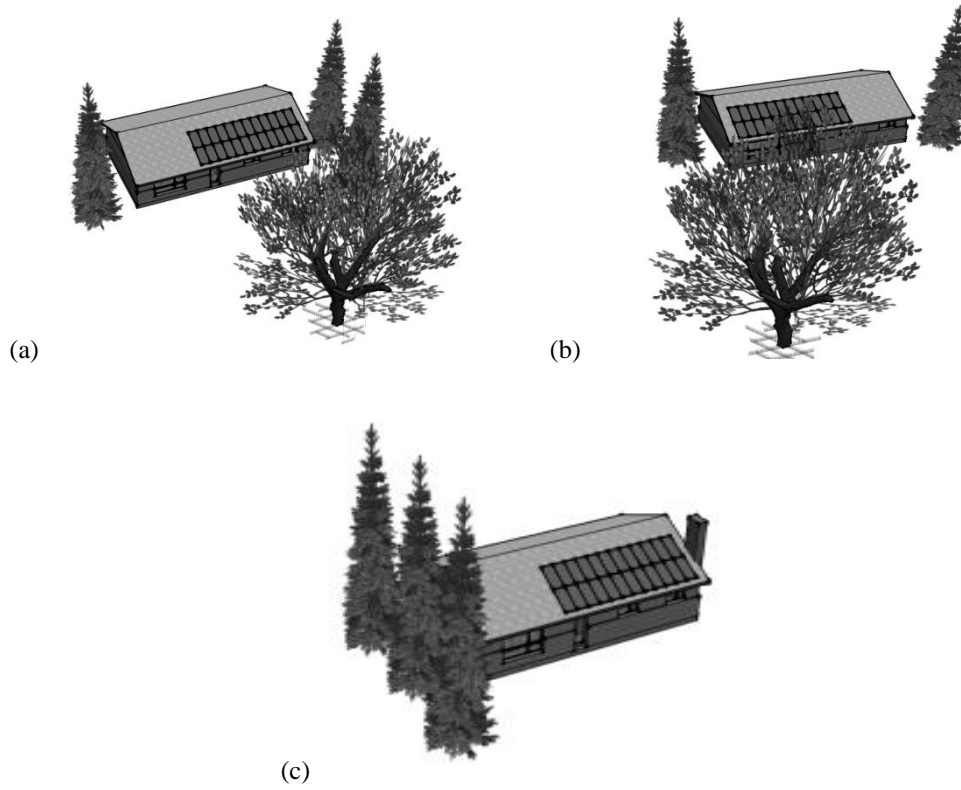
(a)

(b)

(c)

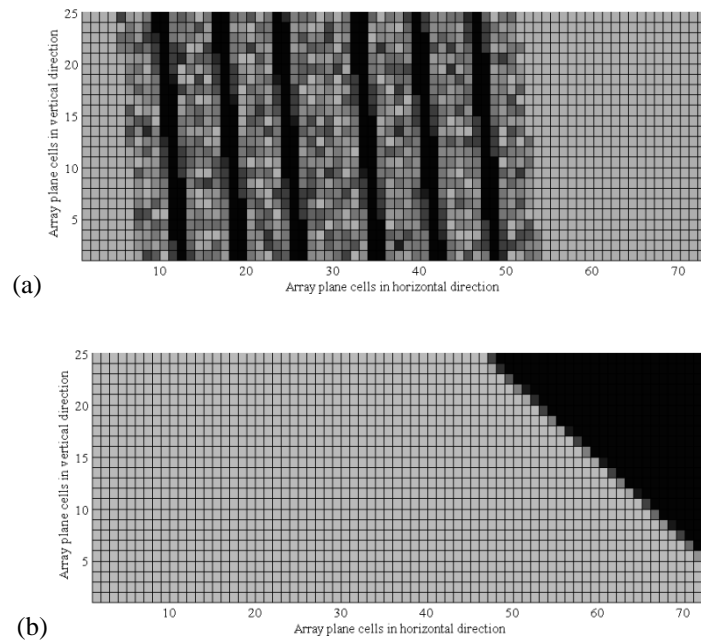**Figure 11 - Shading scenarios: (a) heavy, (b) moderate and (c) light**

(a)

(b)

Figure 12 - Shading mapped onto the array at the cell level for (a) deciduous tree and (b) pine tree

V. RESULTS & ANALYSIS

A. Shading Losses

The light, moderate, and heavy shading cases address the way that the amount of shade on the array affects annual

energy losses and the potential benefits of power optimizers, but do not directly depict the influence of shade

position on the array. In order to better understand the degree of variability in shading losses, the array was

additionally simulated with its strings divided in the two different ways in Figure 14, top-bottom, and left-right, for

the different amounts of shading in Boulder and Orlando. Comparisons of the annual power loss caused by partial

shading are shown for these twelve cases in Table 1.

(a) (b)

Figure 13 - Array configured in (a) top-bottom or (b) left-right strings

Table 1 - Annual shading losses

	Annual % Light Lost	System % Energy Loss	
		top/bot strings	side strings
Denver Heavy	13.7%	32.5%	29.6%
Denver Moderate	6.6%	18.7%	16.6%
Denver Light	3.8%	8.3%	9.7%
Orlando Heavy	9.5%	24.9%	22.1%
Orlando Moderate	4.2%	13.7%	11.9%
Orlando Light	3.2%	8.3%	9.0%

These annual shading losses show two interesting trends. First, shading losses do depend on array configuration;

they are greater for the top-bottom string division in the heavy and moderate shading cases, and greater for the left-

right string division when shading is light. While the differences are only as much as a few percent, they are still

significant because in each case the differences account for ~10% of the total loss. This is attributed to the shade

patterns and the way that they are distributed on the panels, rather than the level of shading on the array, and clearly

shows the importance of detailed modeling of partially shaded systems.

Second, the energy losses from shading are much greater than the amount of light lost, i.e. blocked by the shading obstacles, over the course of the year. Previous works such as [14] have discussed a shade impact factor (SIF) based on the fraction of the array's area that is shaded. In this work, we define the SIF in terms of annual energy loss and annual light loss, as in Equation 8. SIF=1 would indicate ideal shaded operation of the array, with the energy output directly correlated with the amount of available radiation. In all of the cases above, the SIF varies from ~2-3, indicating substantial opportunities for increased energy capture with DMPPT.

$$ \text{SIF} = \frac{\%\ \text{Annual Energy Loss}}{\%\ \text{Annual Light Loss from Shading}} \tag{8} $$

B. Annual Energy Gain Potential

The annual energy gain potential for power optimizers and DMPPT at different levels in the array (string, panel, sub-module, and cell) is shown in Table 2. Only results for the top-bottom string division described previously are included in this table; results for the left-right division were similar, with slightly less potential for the moderate and heavy shading cases, and more for the light shading case (unshaded was unchanged). Both the shaded and unshaded scenarios show generally greater potential in a sunny climate (Boulder) than a cloudy climate (Orlando), indicating less benefit from DMPPT under overcast conditions. Without shading, power optimizers show little advantage; the electrical mismatch between sub-modules of the modeled array creates the opportunity for energy gains of <1%.

Table 2 - Annual energy gains

	Annual % Energy Gain			
	string	panel	sub-module	cell
Denver Heavy	1.6%	16.3%	18.2%	29.7%
Denver Moderate	0.8%	9.3%	10.4%	16.7%
Denver Light	0.9%	3.4%	4.1%	7.2%
Denver Unshaded	0.1%	0.7%	0.8%	---
Orlando Heavy	1.4%	12.5%	13.9%	20.8%
Orlando Moderate	0.7%	6.7%	7.5%	11.5%
Orlando Light	0.9%	3.7%	4.4%	6.8%
Orlando Unshaded	0.1%	0.6%	0.7%	---

The shaded cases show a variety of potential gains, depending on amount of shading and the granularity of power optimizers in the array. While the string level shows limited opportunity for DMPPT, gains of 3.4%-16.3% at the

panel level are significant. Sub-module optimizers show a slight advantage over those at the panel level (~1-2%), but may still be an attractive option if they allow use of lower voltage parts, since they could easily be put in a panel junction box. As expected, cell level DMPPT shows the highest benefit (6.8%-29.7%), nearly twice that of the panel level; however, current PV panel designs and cost considerations may make this approach impractical. It is also important to note that these percentages represent the potential for increased energy using ideal DMPPT; efficiency and insertion losses associated with actual power optimizer designs may decrease gains, though other mismatch factors not considered in this study, such as soiling or temperature variation over the array, may help to balance out any device-specific losses.

C. Recovery of Energy Losses

Percent annual energy gains are a fairly straightforward way of looking at the potential energy gain from power optimizers, but they can span a wide range of values, depending shading extent and other factors, and are often not presented with accompanying system information to aid in their interpretation. This section examines a different metric, percent shade loss recovered (Equation 9), which relates the power recovered to the initial shade-related losses experienced by the PV system.

$$\% \text{ Shade Loss Recovered} = \frac{(\text{Optimized Shaded Energy} - \text{Shaded Energy})}{(\text{Unshaded Energy} - \text{Shaded Energy})} \qquad \textbf{(9)}$$

This metric was examined for DMPPT at the panel level, and results are displayed in Table 3. Results indicate that for all of the simulated shading scenarios, it is possible for power optimizers to recover 34% - 42% of the energy lost from partial system shading. Viewing the potential for energy recovery in this way would allow anyone whose has estimated system shading losses to be able to quickly approximate power optimizer benefits and determine whether or not to consider their use.

Table 3 - Annual loss recovery

	Annual % Light Lost	Annual % Loss Recovered
Denver Heavy	13.7%	33.8%
Denver Moderate	6.6%	40.7%
Denver Light	3.8%	38.1%
Orlando Heavy	9.5%	37.6%
Orlando Moderate	4.2%	42.2%
Orlando Light	3.2%	41.2%

V. CONCLUSION

In conventional grid-tied PV arrays, non-uniform operating conditions can have a disproportionally large impact on system performance, which creates an opportunity for increased energy capture in systems that employ sub-array distributed power conversion and power point tracking (power optimizers). Existing PV modeling tools do not have the level of detail required to accurately model mismatch-related power losses at the system level, making it difficult to estimate the actual potential for power optimizers to boost energy harvest in realistic PV systems. This work has demonstrated an improved methodology for accurate prediction of partial shading and electrical mismatch related losses in PV arrays. The methodology was then used to quantify the device-independent potential for increased annual energy capture in a diverse set of realistic PV installations employing DMPPT at various sub-array levels.

The authors have developed a detailed, flexible annual simulation model for PV systems, which accounts for variations in irradiance and temperature at the PV cell level. This tool allows accurate modeling of both partial shading and varied electrical characteristics between an array's PV generators, as well as the opportunities that mismatch-associated losses create for recoverable power. A typical, residential-sized array was chosen for simulation, configured in two parallel strings. Partial shading of the array was simulated for light, moderate, and heavy shading cases; these were created using a survey of shading found in real, installed PV systems. Emphasis was also placed on realistic simulation of electrical mismatch; this work is the first to use an existing array's measured variations in sub-module electrical characteristics as a basis for electrical mismatch in an annual, system-level energy model.

In all of the simulations with partial shading, annual energy losses were found to be two to three times as large as the amount of light blocked over the year, indicating that the current and voltage balancing requirements in a conventional grid-tied array do create an opportunity for power recovery with DMPPT. The potential for energy gain in unshaded arrays was <1% for all of the cases, but in shaded arrays it increased to 3-16% for panel-level DMPPT and 7-30% for cell-level DMPPT, with slightly greater opportunities in climates receiving more sun throughout the year. In each of the simulated cases panel-level power optimization was able to recover 34-42% of the energy lost to partial shading.

VI. ACKNOWLEDGEMENTS

REFERENCES

[1] E. Roman, R. Alonso, P. Ibanex, S. Elorduizapatarietxe, and D. Foitia, "Intelligent PV Module for Grid-Connected PV Systems," *IEEE Transactions on Industrial Electronics,* vol. 53, no. 4, pp. 1066-1073, August 2006.

[2] G. Walker, J. Xue, and P. Sernia, "PV String Per-Module Maximum Power Point Enabling Converters," *Australasian Universities Power Engineering Conference*, 2003.

[3] G. Walker and J. Pierce, "Cascaded DC-DC Converter Connection of Photovoltaic Modules," *IEEE Transactions on Power Electronics,* vol. 19, no. 4, pp. 1130-1139, July 2004.

[4] L. Linares, R. Erickson, S. MacAlpine, and M. Brandemuehl, "Improved Energy Capture in Series String Photovoltaics via Smart Distributed Power Electronics," *IEEE Applied Power Electronics Conference and Exposition*, 2009, pp. 904-910.

[5] N. Femia, G. Lisi, G. Petrone, G. Spagnuolo, and M. Vitelli, "Distributed Maximym Power Point Tracking of Photovoltaic Arrays: Novel Approach and System Analysis," *IEEE Transactions on Industrial Electronics,* vol. 55, no. 7, pp. 2610-2621, July 2008.

[6] R. Erickson and A. Rogers, "A Microinverter for Building-Integrated Photovoltaics," IEEE *Applied Power Electronics Conference and Exhibition*, 2009, pp. 911-917.

[7] Y. Fang and X. Ma, "A Novel PV Microinverter with Coupled Inductors and Double-Boost Topology," *IEEE Transactions on Power Electronics,* vol. 25, no. 12, pp. 3139-3147, Dec. 2010.

[8] B. Liu, S. Duan, and T. Cai, "Photovoltaic DC-Building-Module-Based BIPV System Concept and Design Considerations," *IEEE Transactions on Power Electronics*, vol. 26, no. 5, pp. 1418 –1429, May 2011.

[9] B. Burger, B. Goeldi, S. Rogalla, and H. Schmidt. "Module Integrated Electronics - An Overview," *25th European Photovoltaic Solar Energy Conference and Exhibition,* 2010, Valencia, Spain.

[10] A. Sanz, I. Vidaurrazaga, A. Pereda, R. Alonso, E. Roman, and V. Martinez. "Centralized vs. Distributed (Power Optimizer) PV System Architecture Field Test Results Under Mismatched Operating Conditions," *37th IEEE Photovoltaic Specialists Conference, 2011,* Seattle, WA.

[11] B. Koirala, B. Sahan, and N. Henze. "Study on MPP Mismatch Losses in Photovoltaic Applications," *24th European Photovoltaic Solar Energy Conference,* 2009, Hamburg, Germany.

[12] D. Picault, B. Raison, and S. Bacha. "Reducing Mismatch Losses in Grid-Connected Residential BIPV Arrays Using Active Power Conversion Components." *European Photovoltaic Solar Energy Conference,* 2010, Valencia, Spain.

[13] E. Roman, V. Martinez, J.C. Jimeno, R. Alonso, P. Ibanez, and S. Elorduizapatarietxe. "Experimental results of controlled PV module for building integrated PV systems." *Solar Energy*, vol. 82, pp. 471-480, 2008.

[14] C. Deline, "Partially Shaded Operation of Multi-string Photovoltaic Systems," *35th IEEE Photovoltaic Specialists Conference,* 2010, Oahu, HI, pp. 394-399.

[15] S. Poshtkouhi, V. Palaniappan, M. Fard and O. Trescases, "A general approach for quantifying the benefit of distributed power electronics for fine grained MPPT in photovoltaic applications using 3D modeling," *IEEE Transactions on Power Electronics*, vol. 99, October 2011

[16] S. MacAlpine, M. Brandemuehl, and R. Erickson, "Potential For Recoverable Power: Simulated Use Of Distributed Power Converters At Various Levels In Partially Shaded Photovoltaic Arrays," *European Photovoltaic Solar Energy Conference,* 2011, Hamburg, Germany.

[17] G. Klise, and J. Stein. *Models Used to Assess the Performance of Photovoltaic Systems.* Albuquerque, NM: Sandia National Laboratories, 2009.

[18] "PVWatts[software]," National Renewable Energy Laboratory, http://www.nrel.gov/rredc/pvwatts.

[19] "System Advisor Model [software]," National Renewable Energy Laboratory, https://sam.nrel.gov/.

[20] "PVsyst [software]", PVsyst SA, http://www.pvsyst.com/.

[21] A. Mermoud and T. Lejeune, "Partial Shadings on PV Arrays: By-Pass Diode Benefits Analysis," *25th European Photovoltaic Solar Energy Conference and Exhibition, 2010,* Valencia, Spain.

[22] "Typical Meteorological Year 3," National Solar Radiation Database, http://rredc.nrel.gov/solar/old_data/nsrdb/1991-2005/tmy3/.

[23] J.A. Duffie, and W.A. Beckman. *Solar Engineering of Thermal Processes.* Hoboken, NJ: John Wiley & Sons, 2006, chapters 1-23.

[24] M. Drif, P.J. Perez, J. Aguilera, and J.D. Aguilar. "A new estimation method of irradiance on a partially shaded PV generator in grid-connected photovoltaic systems." *IEEE Transactions on Renewable Energy*, vol. 33, no 9, pp. 2048-2056, 2008.

[25] D. L. King., W. Boyson, and J. Kratochvil, *Photovoltaic Array Performance Model.* Albuquerque, NM: Sandia National Laboratories, 2003.

[26] T. Neises.,"Modeling Cell Temperature and Performance of Photovoltaic Systems," *Sandia Photovoltaic Modeling Workshop,* September 2010.

[27] M. Boyd., S. Klein, D. Reindl, and B. Dougherty, "Evaluation and Validation of Equivalent Circuit Photovoltaic Solar Cell Performance Models," *Journal of Solar Energy Engineering* , vol. 133, no. 2, May 2011.

[28] IEC, "IEC 61853-1." *"Photovoltaic (PV) module performance testing and energy rating -- Part 1: Irradiance and temperature performance measurements and power rating",* 2011.

[29] S. MacAlpine and M. Brandemuehl. "Photovoltaic Module Model Accuracy at Varying Light Levels and Its Effect on Predicted Annual Energy Output." *37th IEEE Photovoltaic Specialists Conference,* 2011, Seattle, WA.

[30] "Sunny Boy 5000-US," SMA, datasheet, http://files.sma.de/dl/4752/SUNNYBOY5678-DUS120731W.pdf.

[31] BEW Engineering, Inc, "Draft Evaluation Approach for Shade Impact Mitigation Devices," prepared for the California Energy Commission, 2009.

[32] C. Podewils,"Ready to work magic," *Photon International,* October 2011.

[33] "SunTex 80 [product]", Phifer Incorporated, http://www.phifer.com/ExtSunControl.aspx.

[34] K. Emery, "Uncertainty Analysis of Certified Photovoltaic Measurements at the National Renewable Energy Laboratory," National Renewable Energy Laboratory technical report, August 2009.

[35] C. Deline, J. Meydbray, M. Donovan, J. Forrest, "Photovoltaic Shading Testbed for Module-Level Power Electronics," National Renewable Energy Laboratory technical report, May 2012.